IEPC-95-123

# RELEASE INTO THE SPACE OF EXCESS HEAT IN THE PERSPECTIVE HIGH POWER PLANTS

I.G.Panevin*, B.N.Baushev**, A.A.Koroteev**
* *Moscow Aviation Institute, Russia*
** *RIAME MAI, Russia*

Analysis of publications shows that the term "advanced power plants" may refer to the following power plants (PP): high-power steam turbine or gas turbine power plants (like SNAP-50), medium-range nuclear PP with thermionic or thermoelectric conversion (like "Topaz" or SP-100) as well as some other types of PP (for example, solar PP with energy concentrators).

For excessive power rejection into space from space power plants (SPP) or thermal control systems of spacecraft (S/C) or their life support systems conventional radiators are used: flow-through radiators (finned tubes through which a liquid or gaseous heat carrier flows) or heat pipes operating in autonomous mode.

The radiator inlet temperature may vary from $T_w$ = 300 to 1200 K. The radiator specific mass dependence from $T_b$ for conventional radiators (both, in-use and advanced) was derived from the American data and is shown on Fig.1.

$$m_b = f(T_b), \quad m_b = \frac{M_b}{Q_b} = C \cdot T_b^{-4}$$

This dependence is described by the formula:

$$m_b = 1.3 \cdot 10^{11}\ T^{-4}\ (kg \cdot T^4)\ kW,$$

which means that the radiator mass per 1 $m^2$ constitutes approximately 13 kg for the entire temperature range

In addition, conventional radiators are sensitive to the meteorite impact.

Over the last years some advanced radiator (like Droplet-Stream Radiator - DSR) developments were begun. The DSR research is being done basically in the USA and in our country. Paper [1] deals with theory fundamentals and calculation methods for DSR using criteria-parameter dependencies which were developed by generalizing the numerical calculation results obtained at MAI.

These calculations, as well as the data from other authors,

indicate that the DSR specific mass ($m_b$) may be 1.5-2 (or even more) times less than that of conventional radiators.

Besides, DSR are practically 100% meteor-proof. Here after there are presented some theoretical materials from [1] and experimental data on droplet generation with jet nozzles obtained at MAI.

A DSR scheme is given on Fig.2 with general designations. The following parameters are introduced:

Droplet concentration:

$$n_r = 1/b^3 = 1/d^3 z^3 \text{ , where } z = b/d_r \text{ .}$$

Droplet micro and macro cross-sections:

$$\sigma_r = f \cdot \pi V_r^2 \text{ , } \quad \Sigma_r = n_r \cdot \sigma_r$$

f - proportionality factor according to the Mie theory.

The stream albedo:

$$\Omega = 1 - \frac{a_r}{I} \approx 1 - \frac{\varepsilon_r}{I}$$

characterizes the flow optical properties.

The stream optical thickness:

$$\tau = \Sigma_r \delta$$

Droplet stream transparency, at the stream optical thickness being $\tau > 1$, is:

$$K_b = Q_b / Q_b^{(\tau=0)}$$

which is determined from numerical calculations (Fig.3).

A DSR parameter is introduced:

$P = P_o \cdot K_b$ ,

$$\text{where } P_o = \frac{18\ \varepsilon_r\ \sigma\ T_1^3}{\rho_r\ C_{pr}} \cdot \frac{L}{U_r d_r} \cdot K_b = P_o K_b$$

This parameter allows to calculate both optically transparent ($\tau=0$, $K_b=1$) and non-transparent ($\tau>0$) droplet flows.

$$T = \frac{T}{T_1} = (P \frac{X}{L} + 1)^{-3}$$

$$T_2 = \frac{T_2}{T_1} = (P + 1)^{-3}$$

radiator's efficiency:

$$\eta_b = \frac{3\,(1 - \bar{T}_2)}{\bar{T}_2^{-3} - 1}$$

radiating power:

$$Q_n = G \cdot C_{pr}(T_1 - T_2)$$

mass of droplets in the stream:

$$M_b = B\ L\ S\ n_r\ \rho_r\ d_r\ \frac{\pi}{6}$$

droplet specific mass:

$$m_n = \frac{M_b}{Q_b} = \frac{\rho_r\ d_r}{G\ \varepsilon_r\ \sigma\ T_1^4\ \eta_b\ K_b}$$

the dependence $\bar{T} = \frac{X}{L}$ for constant P and $\bar{T}_2$ and $\eta_b$ from P is shown on Fig.4.

Droplet temperature profiles in the stream at different distances X(m) from the droplet generator for $\tau = 10$ are presented on Fig.5.

This information allows to comprehensively calculate a DSR at arbitrary conditions.

The droplet vaporability depends on the vapor elasticity $p_y = f(T_r)$, $d_r$ and DSR operation time t.
The evaporation mass rate is:

$$g_n = \rho_n V_n = \frac{P_n}{\sqrt{2\ \pi\ R_n\ T_n}}$$

the relative mass of evaporated liquid is:

$$\Delta\bar{M}_n = \frac{\Delta M_n}{M_n} = G\,\frac{g_n\ t_u}{\rho_r\ d_r}$$

For lead (Pb), with t = 1 year and $d_r$ = 0.2 or 0.02 mm

at $T_r$ = 1000 K $\Delta\bar{M}_n$ = 145% and 1450%

at $T_r$ = 900 K $\Delta\bar{M}_n$ = 1.45% and 14.5%

It is obvious that evaporation losses grow with $T_r$ and decrease with $d_r$.

These issues are discussed in more detail in [1].

## Experimental study of droplet generation.

Square-edged inlet nozzles with cylindrical channels of length l and diameter $d_a$ were used.

Long nozzles with $\bar{l} = \frac{l}{d_a} \geq 1$ feature a continuous flow ($d_a = d_c$) but there was observed a local narrowing of the flow accompanied by the pressure losses due to which the actual exhaust velocity of the jet is lower than the theoretical one:

$$U_n = (\ldots)^{0.5}; U_n = \left( \frac{2\ \Delta p}{\rho_l} \right)^{0.5}$$

To characterize the nozzle operation the velocity drop coefficient $\varphi = \frac{U}{Un}$, jet narrowing coefficient $\varepsilon = \left( \frac{d_c}{d_a} \right)^2$ and nozzle mass flow rate coefficient

$\mu = \frac{G_a}{F_a \sqrt{2\ \rho_l\ \Delta p}} = \varepsilon\varphi$ are introduced.

For long jet nozzles ($\bar{l} \geq 1$) - $\varphi \cong 0.8$; $\varepsilon = 1$. $\mu \cong 0.8$.

For short nozzles ($\bar{l} < 1$) a detachment flow is observed.

Then:

$\varepsilon \cong 0.6 \div 0.64$, $\varphi = 1$, $\mu = 0.6 \div 0.64$

i.e $d_c \cong 0.8\ d_a$ and $U = U_n$;

It has to be mentioned that in case of $\bar{l} \geq 1$ the jet is better centered (compared to the case when $\bar{l} < 0.5$) and droplet collision probability is lower.

Jet collapse has been studied for the streams expelled out into the atmosphere or vacuum. The fluids used were water, vacuum oil and some other liquids. The outflow velocity constituted U ~ 5 m/s. The stream diameter $d_c \geq 0.3$ mm. Studied were both free (Rayleigh's) and induced jet collapse when in the latter case oscillations from an external source were applied to the nozzle body. The stream and droplet formation were spark-photographed (with 1 μs exposure).

Fig.6 and 7 show collapse of 10 parallel streams and Fig.8 that of a single stream with various frequency oscillations (f = 15 and 1000 1/s) applied to the nozzle.

In case of a free (Rayleigh's) stream collapse the oscillations from the fluid feed system affect the jet and the spray appears to be irregular. In case of induced collapse, the spray becomes regular and droplet diameter is determined by the applied frequency f, stream diameter $d_c$ and flow rate U. As f increases, the disturbance wavelength λ decreases in the flow (for

free collapse $\lambda = 4.5\ d_c$):
decrease both the liquid volume per droplet and the droplet size:

$$d_r = d_c \sqrt{1.5\ \bar{\lambda}}$$

$$\text{where } \bar{\lambda} = \frac{\lambda}{d_c} = \frac{U}{d_c} \cdot \frac{1}{f}$$

This relationship was proven experimentally. The collapsing length for solid streams is much less than the DSR length L.

References:

1. I.G.Panevin. High-temperature heat exchangers for spacecraft power plants (theory and calculations of droplet-stream radiators) (in Russian). Moscow, MAI Publishing House, 1990. 62 pages.

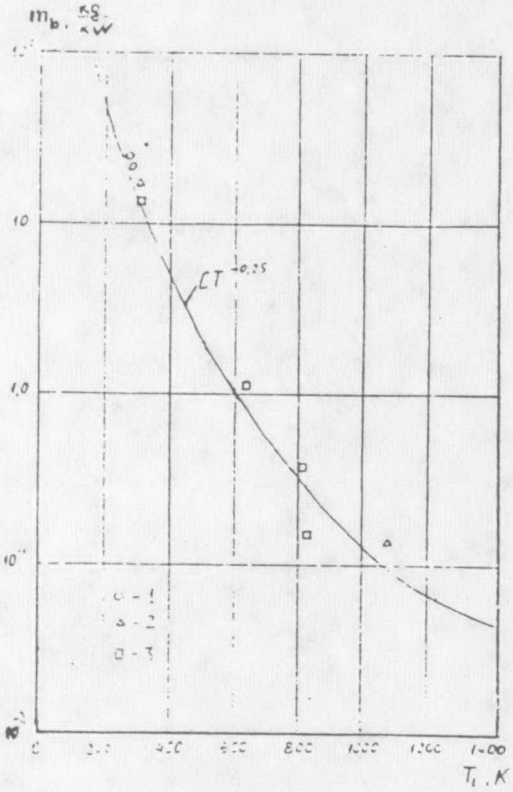


Fig.1.

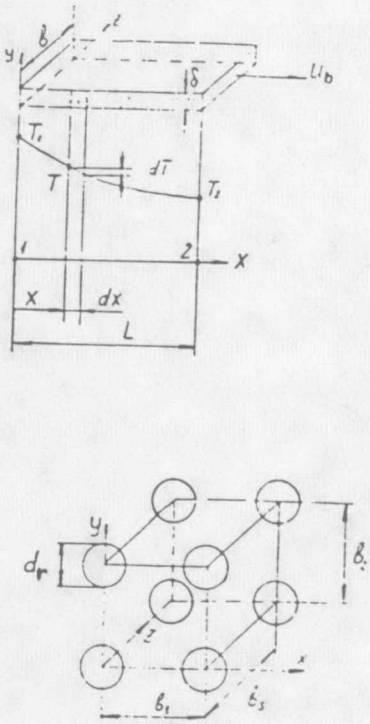


Fig.2.

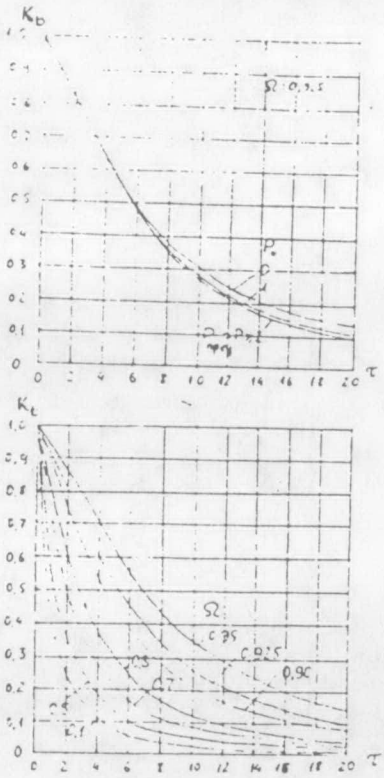


Fig.3.

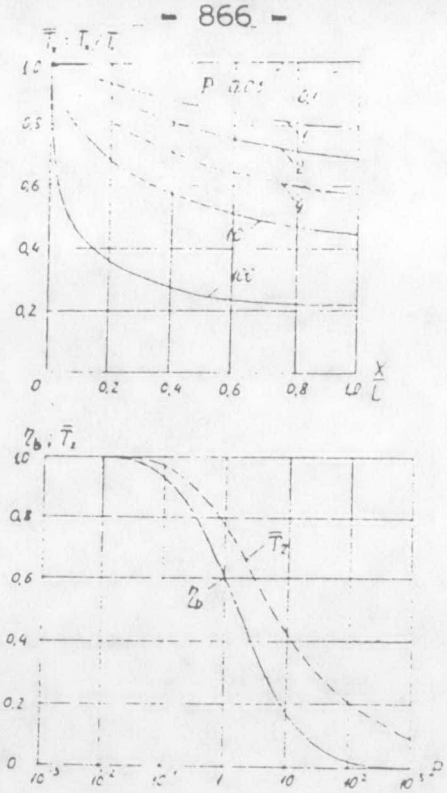


Fig.4.

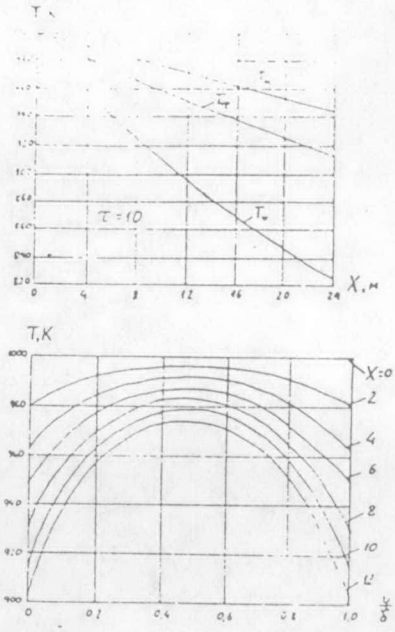


Fig 5.

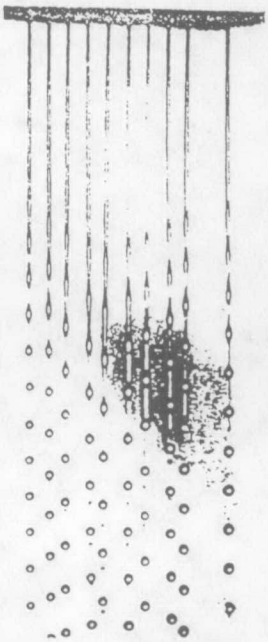

Fig 6.

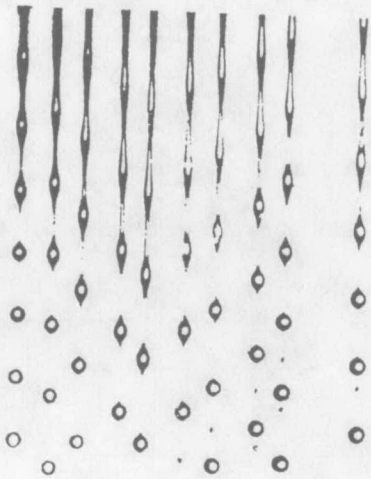

Fig 7

Fig 8

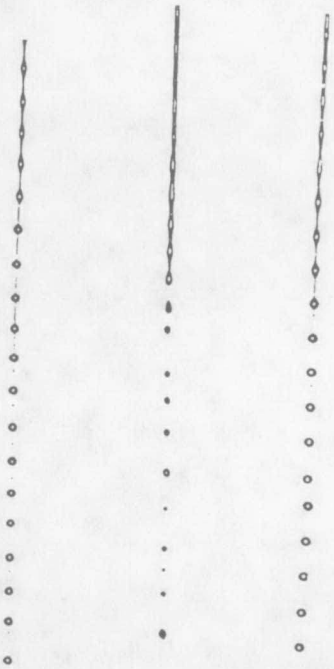

Fig.9